Electronic Supplementary Material (ESI) for Materials Chemistry Frontiers.

Self-Organisation and Characterisation of Hierarchical Structures in Trimethyl β-Cyclodextrin Nano-Films

Shigesaburo Ogawa[a,b], Koji Ashida[c], Tadaaki Kaneko[c], and Isao Takahashi[a]*

***a*. Department of Physics, School of Science and Technology, Kwansei Gakuin University, Sanda 669-1337, Japan.**
***b*. (Present) Department of Materials and Life Science, Faculty of Science and Technology, Seikei University, 3-3-1 Kichijojikitamachi, Musashino-shi, Tokyo, 180-8633, Japan**
***c*. Department of Nanotechnology, Science and Technology, Kwansei Gakuin University, Sanda 669-1337, Japan. E-mail: suikyo@kwansei.ac.jp**

Corresponding author*: E-mails: (I. Takahashi) suikyo@kwansei.ac.jp

Supporting Results

1) Thermal characterisations of bulk trimethyl β-Cyclodextrin

Differential scanning calorimetry (DSC) measurements of commercially received and purified TMCDs in a hermetical aluminium pan were conducted by using a DSC 8500 (PerkinElmer Co. Ltd., USA).

Figure S1 shows DSC heating thermograms of trimethyl *β*-Cyclodextrin (TMCD) powder with and without purification. The melting of two types of crystals is recognised in the heating process for the sample without purification (Fig. S1a), whereas a single melting at 156 °C, which is consistent with that of monohydrate crystal,[44] occurs for that with purification (Fig. S1b). These results indicate that all TMCD samples are monohydrates after purification, while the commercial sample without purification contains several hydrated TMCD states.

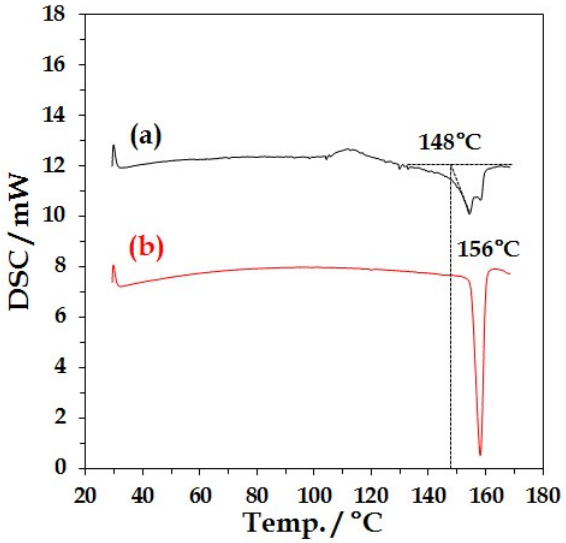

Fig. S1 DSC heating thermograms of TMCD bulk sample (a) as received and (b) after purification.

2) Determination of effective thermal annealing conditions

To achieve the effective crystallisation condition, the isothermal annealing above T_g of TMCD film was carried out. Figure S2a shows the peak intensities of diffraction peaks around 7.64° for PXRD profiles of TMCD films (*ca.* 12 nm) after thermal annealing for 12 h at different annealing temperatures between 96 and 164 °C. Apparently, the thermal annealing around 120 °C effectively induces the molecular assembly of TMCD. In addition, as shown in Fig. S2b, the time evolution of the peak intensities for TMCD films obtained by the same annealing conditions shows that the annealing time of 12 h suffices to complete self-assembly in the nano films with *ca.* 12 nm thickness.

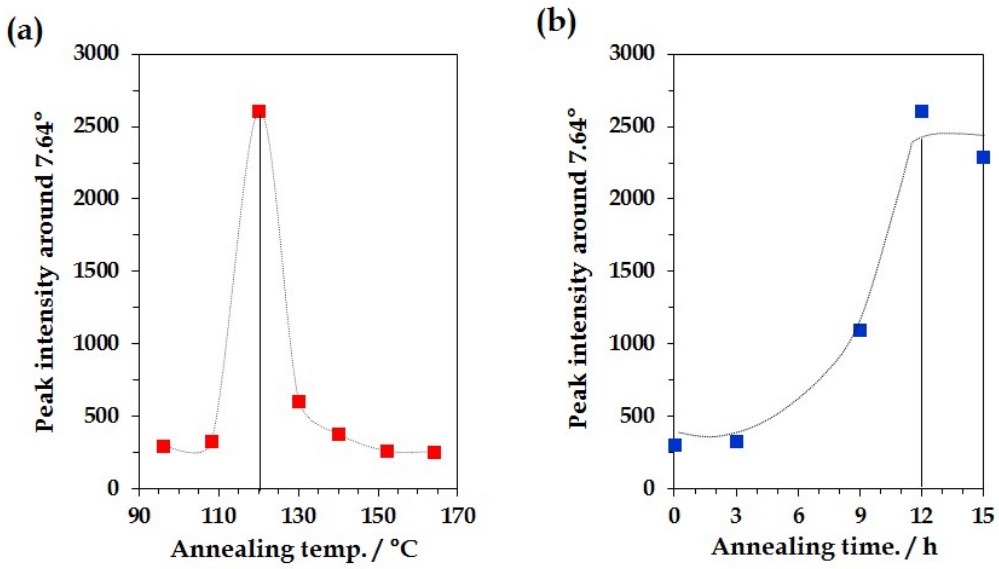

Fig. S2 Peak intensities of the diffraction around 7.64° for PXRD profiles of TMCD films (*ca.* 12 nm) obtained by thermal annealing as a function of (a) temperature with the constant annealing time (12 h) and (b) time with annealing temperature at 120 °C.

3) Assignment of 2D-GIXD profile of TMCD crystal in nanosheet

A 2D-GIXD profile of TMCD crystal in nanosheet form *(ca.* 12 nm) was depicted in Fig. S3. For each diffraction spot labelled alphabetically in Fig. S3, the experimental *d* spacings and the corresponding Miller indices are summarised in Table S1. Here, the regular spacing *d* of the TMCD crystal in nanosheet form was calculated by Bragg's law, $n\lambda = 2d \sin\theta$, while the Miller index assignment for each reflection spot was done by a calculation using the lattice constants reported for TMCD monohydrate,[44] trihydrate,[44] and anhydrous[43] crystals under the conditions that the Miller indices between out-of-plane and in-plane become orthogonal.

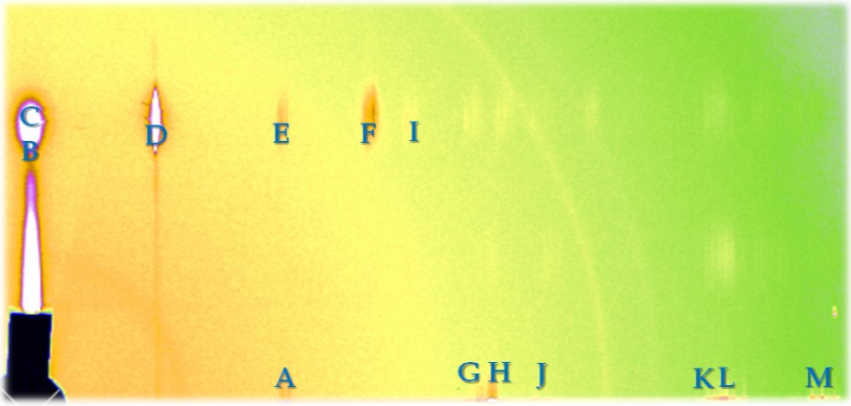

Fig. S3 A 2D-GIXD profile of TMCD crystal in nanosheet (*ca.* 12 nm) at 30 °C.

Table S1 Comparison of representative experimental Bragg spacing for TMCD crystal in nanosheet form and calculated Bragg spacings for TMCD monohydrate, trihydrate, and anhydrous crystals at 30 °C.

Sign	Expt.; in Å	Monohydrate			Trihydrate			Anhydrous			Calcul.; in Å
A	13.4	0	0	2							13.3
B	11.7	1	1	0							11.8
C	11.3				1	1	0	1	1	0	11.5
D	10.6	1	1	1							10.8
E	8.8	1	1	2							8.8
F	7.5				1	1	3				7.6
G	7.5				0	0	4				7.5
H	7.3							0	0	4	7.2
I	7.0	1	1	3							7.1
J	6.7	0	0	4							6.6
K	5.0							0	0	6	5.0
L	4.9				0	0	6				4.8
M	4.4	0	0	6							4.4